Multi-point Cluster observations of VLF risers, fallers and hooks at and near the plasmapause

J. S. Pickett[1], O. Santolík[1,2], S. W. Kahler[1], A. Masson[3], M. L. Adrian[4], D. A. Gurnett[1], T. F. Bell[5], H. Laakso[3], M. Parrot[6], P. Décréau[7], A. Fazakerley[8], N. Cornilleau-Wehrlin[9], A. Balogh[10], and M. André[11]

1 Department of Physics and Astronomy, The University of Iowa, Iowa City, IA, USA
2 Faculty of Mathematics and Physics, Charles University, Prague, Czech Republic
3 RSSD of ESA, ESTEC, Noordwijk, The Netherlands
4 Marshall Space Flight Center, Huntsville, AL, USA
5 Starlab, Stanford University, Stanford, CA, USA
6 LPCE/CNRS, Orleans, France
7 LPCE et Université d'Orléans, Orléans, France
8 Mullard Space Science Laboratory, University College, London, UK
9 CETP/UVSQ, Velizy, France
10 The Blackett Laboratory, Imperial College, London, UK
11 Swedish Institute of Space Physics, Uppsala Division, Uppsala, Sweden

Abstract

The four Cluster Wideband (WBD) plasma wave receivers occasionally observe electromagnetic triggered wave emissions at and near the plasmapause. These triggered emissions usually consist of very fine structured VLF risers, fallers and hooks in the frequency range of 1.5 to 3.5 kHz with frequency drifts for the risers on the order of 1 kHz/s. They appear to be triggered out of the background whistler mode waves (hiss) that are usually observed in this region, as well as from narrowband, constant frequency emissions. Occasionally, identical, but weaker, emissions are seen to follow the initial triggered emissions. When all the Cluster spacecraft are relatively close (< 800 km, with interspacecraft separations of around 100-200 km), the triggered emissions are correlated across all the

spacecraft. On Cluster the triggered emissions are usually observed near perigee (around 4-5 R_E) within about 20 degrees, north or south, of the magnetic equator at varying magnetic local times and generally at times of low to moderate Kp. In at least one case they have been observed to be propagating toward the magnetic equator at group velocities on the order of 5-9 x 10^7 m/s. The triggered emissions are often observed in the region of steep density gradient either leading up to or away from the plasmasphere where small-scale density cavities are often encountered. Through analysis of images from the EUV instrument onboard the IMAGE spacecraft, we provide evidence that Cluster may sometimes be immersed in a low density channel or other complex structure at the plasmapause when it observes the triggered emissions. Examples of the various types of triggered emissions are provided which show the correlations across spacecraft. Supporting density data are included in order to determine the location of the plasmapause. A nonlinear gyroresonance wave-particle interaction mechanism is discussed as one possible generation mechanism.

1. INTRODUCTION

Triggered and discrete narrowband emissions have been observed on the ground and in space for decades [Smith and Nunn, 1998]. These emissions are generally observed both inside and outside the plasmapause at L values ranging from about 2.5 to 10. They are observed primarily in the form of risers, fallers and upward and downward hooks, or combinations thereof (cf., Helliwell, [1965];

Smith and Nunn, [1998]). Discrete emissions have been defined as emissions having no obvious trigger source, whereas triggered emissions have a clearly recognizable trigger signal [Nunn et al., 1997]. A review of the observations and generation theories of triggered emissions was contained in Matsumoto [1979] and Omura et al. [1991] who characterized these emissions as 1) being narrow bandwidth, usually less than 100 Hz; 2) having long durations, sometimes on the order of 1 s; 3) having large amplitudes which saturate at a level as much as 30 dB above that of the triggering signal; 4) having continuously sweeping frequency, typically at a rate of order kHz/s; and 5) taking place almost always within the plasmasphere. Triggered emissions are observed to be produced by constant-frequency wave (CW) transmissions from terrestrial VLF transmitters [Helliwell, 1965; Bell, 1985], by lightning VLF whistlers [Nunn and Smith, 1996], by magnetospheric lines and strong Power-Line Harmonic Radiation (PLHR) induction lines [Nunn et al., 1997] and by hiss [Smith and Nunn, 1998].

Discrete emissions have similar characteristics as triggered emissions but appear as isolated events, perhaps arising spontaneously because of high instability conditions in the plasma triggered by random noise, very weak PLHR, or unducted VLF signals [Nunn et al., 1997]. They can be either ducted or unducted. VLF chorus is composed of a sequence of closely spaced, discrete emissions, often overlapping in time and most often consisting of rising tones [Helliwell, 1965]. Thus chorus shares many of the characteristics of the more isolated discrete emissions. Often a background of hiss is present when chorus

is observed. For a review of chorus observations and theory, see Sazhin and Hayakawa [1992].

Several more recent studies have been published that deal with triggered, discrete and chorus emissions. These include, but are not limited to, LeDocq, et al. [1998], Trakhtengerts [1999], Bell et al. [2000], Trakhtengerts and Rycroft [2000], Meredith et al. [2001], Pasmanik, et al. [2002], Lauben et al. [2002], Santolík and Gurnett [2003], and Parrot et al. [2003]. Several studies are ongoing at the present time to help provide further understanding of the propagation characteristics of these emissions, as well as their generation mechanisms. For example, one surprising aspect of chorus was the discovery by Gurnett et al. [2001] that correlated chorus elements appear at different frequencies on the various Cluster spacecraft separated by distances of a few hundred km or less.

The main aim of this paper is to bring a multi-spacecraft perspective to the observations of triggered emissions in the form of risers, fallers, hooks and combinations thereof that are made on Cluster at and inside the plasmapause. We refer to these emissions as triggered emissions as they appear in many cases to be triggered from observable wave sources. In a few of the cases where the triggering emission is somewhat in doubt, the emissions might better be referred to as discrete since the individual risers, fallers and hooks are well isolated from one another. We begin by describing the suite of instruments on

the Cluster and IMAGE spacecraft whose observations are the focus of this study. We show examples of the types of triggered emissions that are observed and their correlation across several spacecraft separated by hundreds of km. This is followed by a discussion of the observations in terms of their significance and of a possible generation mechanism.

2. INSTRUMENTATION

The primary observations discussed below are from the Cluster Wideband (WBD) plasma wave receiver [Gurnett et al., 1997] which makes a one-axis measurement of the electric or magnetic field using one spin plane, 88 m dipole antenna or one of three magnetic searchcoils. WBD continuously samples waveforms using a 9.5 kHz bandwidth filter with filter roll-off occurring at about 50 Hz on the low end and 9.5 kHz on the high end. It contains an automatic gain system, implemented in hardware, with gain update rate of 0.1 s, which helps to keep the high intensity triggered emissions within the dynamic range of the instrument without clipping. The data are sampled at high time resolution, 36.5 μs, by transmitting the data directly to the Deep Space Network (DSN) ground stations located in Canberra, Australia and Goldstone, California, USA. WBD data on each spacecraft are obtained over approximately 4% of any one 57-hour Cluster orbit. All of the WBD data shown in this paper were obtained while the spacecraft were near perigee (4.0-4.5 Re). Typically, in this region of space WBD cycles between an electric antenna and a magnetic searchcoil antenna

with a 42s/10s duty cycle, respectively. Since the onboard time counter only allows for absolute time accuracy to about 2 ms, WBD makes use of the ground receive time tags provided by DSN, which are accurate to 10 μs, in order to determine time delays between spacecraft.

In situ density measurements are obtained by the Whisper sounder [Décréau et al., 1997], provided the plasma frequency associated with that density is less than 80 kHz. The Whisper sounder is designed to provide an absolute measurement of the total plasma density by means of a resonance sounding technique in the range of 0.2 – 80 cm^{-3}. These measurements are usually made for a period of about 3 s every 52 s during WBD operation. The EFW instrument measures electric fields and waves with two pairs of probes on wire booms in the spin plane of each satellite (the same probes used by WBD to make its wave electric field measurements). Each pair has a probe-to-probe separation of 88 m [Gustafsson et al., 1997]. The potential of the probes with respect to the spacecraft is sampled at 5 samples/s, and this measurement can be used to estimate the plasma density in all but perhaps the most tenuous magnetospheric plasmas traversed by Cluster where the technique may break down due to the spacecraft current balance being more sensitive to the energy of the ambient electrons [Pedersen et al., 2001, André et al, 2001]. The lower time resolution density measurements from the Whisper Sounder have been used here to better calibrate the density values obtained from the higher time resolution EFW potential measurements. Simultaneous measurements of the waves using the

two spin plane electric field antennas and the three magnetic searchcoils at frequencies up to 4 kHz are made by the STAFF-SA instrument [Cornilleau-Wherlin, 1997]. STAFF-SA provides the complete auto- and cross-spectra over a frequency range of nine octaves, which are then analyzed to obtain the wave vector, Poynting vector, ellipticity and planarity of polarization. The magnetic field measurements that are used to calculate the electron cyclotron frequency and to determine each of the spacecraft's locations in a magnetic field aligned coordinate system are provided by the FGM instrument [Balogh et al., 1997]. FGM consists of two triaxial fluxgate magnetometers, with one of the sensors located at the end of one of the two 5.2 m radial booms of the spacecraft and the other at 1.5 m inboard from the end of the boom. Remote sensing of the plasmasphere is provided by the Extreme Ultraviolet Imager (EUV) located on the IMAGE spacecraft [Sandel et al., 2000]. EUV is designed to image the distribution of plasmaspheric He^+ ions (typically plasmaspheric He^+/H^+ ~ 0.1-0.2) via resonant scattering of solar 30.4-nm UV radiation. Tuned specifically to detect the 30.4-nm resonance line of plasmaspheric He^+, EUV consists of three wide–field (30°) cameras such that the field–of–view (FOV) of the three cameras overlap slightly to form a fan–shaped instantaneous FOV of dimensions 84° x 30° (Sandel et al., 2000; 2001). As the IMAGE satellite proceeds through a single spin, the fan–shaped FOV of EUV sweeps across an 84° x 360° swath of sky recording the intensity of detected 30.4-nm radiation in an array of approximately 0.6° x 0.6° pixels. Since the plasmaspheric He^+ scattered 30.4-nm emission is an optically thin medium, the measured intensity is directly proportional to the

He^+ column density along the line of sight through the plasmasphere. Each frame of EUV imaged data is produced from a 10-minute accumulation that encompasses 5–spins of the IMAGE satellite.

3. OBSERVATIONS

We present WBD observations of triggered emissions in the form of VLF risers, fallers and hooks from three different dates, March 11, 2002, June 23, 2003 and August 31, 2003, when Cluster was located at or near the plasmapause. The Kp index for each of these three dates was moderate to low at 2-, 4, and +1, respectively. The Kp index is probably important as it is based on processes that have been shown to affect the location of the plasmapause [Moldwin et al., 2002].

3.1 March 11, 2002

We begin our survey of the triggered emissions by showing an example from March 11, 2002 when the four spacecraft were relatively close to each other (~100 km separations). Figure 1 is a typical frequency, in kHz, vs. time, in UT hours:minutes:seconds, spectrogram with gray scale indicating electric field power spectral density. The panels from top to bottom show the WBD data from Cluster spacecraft (SC) 1 through 4, respectively. This particular example spans a time period of 4 seconds in which triggered emissions in the form of linked

risers and fallers, or upward and downward hooks, are observed to form a nearly sinusoidal signature in the frequency domain. The triggered emissions span the frequency range of about 2.5-3.5 kHz and appear to be triggered out of a narrowband, nearly constant frequency emission observed at about 2.8 kHz. The triggered emissions are well-correlated across all four spacecraft. One particularly interesting feature of these triggered emissions is their reappearance, suggestive of reflection of the principal emission, approximately ½ s after the initial principal intense emissions, but at a much reduced amplitude and slightly more diffuse. These data were obtained while the spacecraft were at 4.4 R_E, 19.3º magnetic latitude, 23.3 hours magnetic local time and 4.9 L-shell. Although not shown in Figure 1, WBD data obtained just prior to 07:45:00, while the instrument was sampling with the magnetic searchcoil as a sensor for 10 s, clearly show that the triggered emissions have magnetic components where the E/B ratio is higher for the waves from which the emissions are triggered than for the triggered emissions themselves. In addition, the overall intensity of the triggered emissions is much higher than the waves from which they are triggered.

The in situ density profile for this March 11, 2002 triggered emission case is shown in Figure 2. This profile was obtained from combining the Whisper sounder and EFW spacecraft potential measurements. The top panel shows density, in cm^{-3}, vs. time, in decimal hours UT, color-coded by spacecraft, for the entire plasmasphere crossing by Cluster on this orbit. The bottom panel shows a higher resolution view of the density during exit from the plasmasphere at 07:45

to 07:50 UT. The triggered emissions seen in Figure 1 were observed during plasmasphere exit in the plateau region at a density around 70 cm^{-3}. For this pass, the triggered emissions are observed primarily only in the plateau region right after the density has made its initial drop up to the time that the small density cavities are observed to begin just after 07:46 UT and then again during the time of the major density cavities from 07:47 to 07:49.

An image of the plasmasphere taken by the IMAGE EUV instrument not long after the Cluster measurements shown in Figure 1 shows a complex plasmapause region that contains an inner and outer wall of an embedded low-density channel (see Figure 3a). When these image data are co-rotated back to the time of the Cluster measurements, we see in Figure 3b, right-hand panel, that Cluster is immersed in this complex structure at the plasmapause consistent with the density data observed in situ by Cluster (Figure 2).

3.2 June 23, 2003

Next we turn to an example of some well-isolated risers and hooks observed on June 23, 2003 when the Cluster spacecraft were in the middle of their major maneuver period of going from large spacecraft separations (order of 5,000 km) to their small separations (order of 200 km). At this time the two pairs of spacecraft (1,3 and 2,4) were separated by about 10,000 km, while the distances between the two spacecraft in each pair were on the order of 360 km. Because

of the large distance between the two pairs, we resort to showing only the data from one pair (2 and 4) in order to observe the correlation of the triggered emissions. Figure 4 is a spectrogram in the same format at Figure 1 showing the WBD data from these two spacecraft while they were at 4.4 R_E, 12.1º magnetic latitude, 16.8 hours magnetic local time and 4.6 L-shell. Clearly, the isolated riser/hook combinations are correlated between the two spacecraft in the frequency domain, although the riser/hook combinations are considerably more intense on SC2. This suggests that the source may be closer to SC2. The frequency range of these emissions is about 2 to 3.5 kHz and their frequency drift is on the order of 1 kHz/s. In this case the riser/hook combinations appear to be triggered out of the low frequency waves (hiss) that cover the frequency range from the lowest frequency measured (about 50 Hz) up to about 2 kHz. Note also the presence of secondary triggered emissions from the risers, some of which are seen only on one spacecraft, such as the one centered at 03:45:13 UT on SC4.

In order to determine the direction of propagation of these isolated riser/hook combinations, it is necessary to go to the time domain to do the analysis since the spectrograms are created using FFTs which average over time scales much larger than the delay times. We have chosen the riser/hook centered on 03:45:13 UT for our analysis. Figure 5 shows the filtered waveforms for 0.5 seconds beginning at 03:45:13 UT. Plotted on the vertical axis are the calibrated electric field amplitudes, in mV/m, of the waveforms vs. time, in s, obtained by

WBD on SC2 (top panel) and SC4 (bottom panel). This figure makes it clear that SC2 observes higher amplitude waves than SC4 as stated above. We have chosen to use a Finite Impulse Response (FIR) filter over the 2-3 kHz frequency range in order to remain outside the frequency range of the intense low frequency waves and yet fully contain a major portion of the riser portion of the triggered emission. We have pointed out four different correlated wave packet intervals for further analysis by putting a grey-shaded box around them and numbering them 1 through 4 in each of the two panels. For each of the four chosen wave packets we have calculated a delay time of arrival at SC4 from SC2 using the peaks as our reference. The results of these calculations are shown in Table 1. Notice that the delay time, which varies from about 3 to 4.5 ms, decreases with time. Events 1 and 2 are from a time when the riser frequency is increasing. Events 3 and 4 are from a time after the peak of the hook when frequency is starting to decrease slightly. Although the spacecraft are getting closer to each other at this time, the closing distance is not sufficient to account for the decreasing delay times. The error in the time measurement is also not sufficient to account for the decreasing delay times. At this time SC2 is farther from the earth than SC4. SC2 is also at higher magnetic latitude than SC4. Since SC2 observes the wave packets first, the group velocity of this riser-hook combination must have a positive projection in the direction of the SC2-SC4 separation vector, i.e., in the direction toward the Earth and toward the magnetic equator. The same is true for the other risers/hooks observed in Figure 4. Based on the separation distance along the direction of the magnetic field as

shown in Table 2 and the delay times shown in Table 1, and an assumption that these electromagnetic triggered emission waves are traveling along, or nearly along, the local magnetic field, we find that their group velocity is on the order of 6-9 x 10^7 m/s directed toward the magnetic equator. Cold plasma theory predicts for a wave of this frequency a group speed of 2 x 10^7 m/s [Stix, 1992].

The density profile for this encounter is shown in Figure 6 and is annotated using the ephemeris of Cluster 2. Whisper sounder data together with EFW spacecraft potential measurements have been used to obtain a density, plotted in cm^{-3} along the vertical axis, vs. time, in hours:minutes along the horizontal axis. The two traces are color coded by spacecraft. The density values clearly indicate that the Cluster spacecraft encountered a commonly observed localized region of highly–structured dense plasma in the local time sector ~1600–1700 MLT between 4–7 R_E [Moldwin et al., 1994]. The time of the riser/hook combination observations by WBD is indicated by an arrow, and is consistent with the spacecraft being located within one of the several broader localized density cavities within this localized region of dense plasma, even though SC2 is embedded in a narrower localized density enhancement.

The STAFF-SA data that cover the time period of the risers observed by WBD are shown in Figure 7. We show the data of SC2 where the emissions are more intense. The data of SC4 are not shown but lead to similar results. The upper two panels demonstrate that both the hiss below 2 kHz and triggered

emissions between 2 and 3 kHz are electromagnetic waves, the intensity of hiss being modulated by density enhancements seen in Figure 6. Additional analysis shows that the waves are right-hand polarized consistent with their propagation in the whistler mode (not shown). Panel (c) represents results of analysis of the wave vector direction using singular value decomposition (SVD) of the magnetic cross-spectral matrix [Santolík et al., 2003]. The wave vector of the hiss and triggered emissions is found to be within 20-30 degrees of the direction of the stationary magnetic field. Panel (d) shows the electromagnetic planarity estimator [Santolík et al., 2003] indicating if the waves propagate close to one single direction (values close to 1) or if the energy is distributed between antiparallel wave normals (values close to 0). The results correspond to wave vectors close to one single direction for the hiss and triggered emissions. Finally, panel (e) shows the component of the Poynting flux parallel to the stationary magnetic field normalized by its standard deviation [Santolík et al, 2001]. Positive values (red) obtained for the hiss and triggered emissions signify that these waves propagate approximately in the direction of the stationary magnetic field, i.e., from the magnetic equator toward higher magnetic latitudes. For some cases of short-duration triggered emissions at higher frequencies, however, we cannot exclude opposite propagation since the results are not statistically reliable (green).

3.3 August 31, 2003

As a final example, we show in Figure 8 a series of correlated risers, centered at 2 kHz, that were observed on August 31, 2003 at around 02:25 UT and that range in frequency from about 1.5 kHz up to about 2.5 kHz with frequency drifts on the order of 1 kHz/s. They appear to arise out of a lower frequency hiss-type emission whose upper cutoff frequency is about 1.8 kHz and extend up into a band of more structured emission centered at about 2.9 kHz. Note also the secondary triggers coming off some of the risers, e.g., at 02:25:04 UT and the presence of a sinusoidal-shaped trigger starting around 02:25:07 UT, similar to those observed on March 11, 2002. The risers observed on August 31, 2003 appear to be triggered out of the diffuse plasma waves observed over the frequency range of 200 Hz to 1.8 kHz and be weakest on SC1 (perhaps furthest from source).

On this date the four spacecraft were located at approximately 4.6 R_E, -19.3º magnetic latitude, 12.5 hours magnetic local time and L-shell of 5.2 The density profile shown in Figure 9 (same format as Figure 6, but using the ephemeris of Cluster 1) indicates that these triggered emissions were observed during entry into a post–noon localized, highly–structured region of dense plasma [Chappell et al., 1971] with the emissions occurring in the region of steepest density gradient (see arrow).

4. DISCUSSION

The Cluster WBD instrument has obtained multi-spacecraft measurements of the various types of triggered and discrete emissions that have long been observed on the ground and in space by one spacecraft. Upward and downward hooks, or linked risers and fallers, of the type shown in Figure 1 look very similar to those obtained at Halley station, Antarctica shown in Figure 1(e) of Smith and Nunn [1998]. Likewise, the risers with downward hooks that arise out of the hiss as shown in Figure 4 look very similar to those which rise out of the hiss as shown in Figure 1(g) of Smith and Nunn [1998]. Using the Cluster multispacecraft capability, we have found that the triggered and discrete emissions are often observed to be correlated across distances as great as 800 km across and along the magnetic field direction. Santolík and Gurnett [2003] found a significant correlation at distances of a few hundred km, but the correlation coefficient decreased with a characteristic scale of ~100 km across the magnetic field direction. They used WBD chorus data obtained under disturbed (high Kp) conditions in the low density region outside the plasmapause. Thus, it appears that correlation distances may be shorter outside the plasmapause than inside based on these two studies. Statistical studies of these correlation lengths have now been started in order to determine what these correlation lengths are, both inside and outside the plasmapause, and the dependence, if any, on solar wind pressure and interplanetary magnetic field configuration.

Another characteristic of the triggered emissions discussed in this study is that they sometimes propagate toward Earth and the magnetic equator as observed on June 23, 2003. Chorus has generally been shown to propagate away from the equator [LeDocq et al., 1998], although Parrot et al. [2003] have shown that there is a reflected component of chorus that propagates back toward the equator after lower hybrid resonance reflection. Likewise, the reappearance on March 11, 2002 of the triggered emissions at much lower intensity approximately ½ s after the appearance of the principal triggered emissions observed by Cluster suggests that a series of linked upward and downward hooks may also be reflected. Supposing a constant group speed of 2×10^7 m/s obtained from the cold plasma theory, the delay of 0.5 s gives a rough estimate of the distance of ~1 Earth radius to a reflection point. Future research will attempt to identify the location of the reflection point using a ray tracing algorithm.

The difference in the group velocity obtained for the riser/hook combination on June 23 2003 and that obtained from cold plasma theory is still under investigation. The error in the time delay measurements could not account for this difference. The possibility exists that there may be a warmer particle population embedded in this highly-structured, generally cold plasmaspheric plasma which could account for this difference in the measured velocity to the theoretical one. Analysis of future events with simultaneous particle measurements should help resolve this problem. In addition, the reason for the

trend observed on the same date of decreasing time delays with time for the riser/hook combinations is also still under investigation. A Doppler shift could not account for this trend since the average phase speeds of the triggered emissions is on the order of 1.5×10^7 m/s.

Regarding a generation mechanism for the triggered emissions observed on Cluster, we have briefly explored the generation mechanism proposed by Bell et al. [2000] for triggered emissions observed on Polar inside the plasmasphere. This generation mechanism involves a nonlinear gyroresonance interaction between the energetic electrons and the VLF waves, which in the Cluster case would be VLF hiss and constant-frequency emissions. A cursory analysis of the Cluster PEACE [Johnstone et al., 1997] electron data suggests that there may be enough amplification of the waves as they propagate across the magnetic equator in the presence of 15-26 keV electrons to produce the triggered emissions. However, analysis of these data have literally just begun on Cluster for these types of studies since PEACE electron data have just started (in mid 2003) to be taken consistently through Cluster perigee. Thus, there is much work still ongoing in this area.

5. SUMMARY AND CONCLUDING REMARKS

A summary of our main findings with respect to triggered emissions observed on Cluster multi-spacecraft at or near the plasmapause using the Wideband plasma wave receiver as a detector is as follows:

- The VLF triggered emissions are observed on Cluster as electromagnetic fine-structured risers, fallers, hooks and combinations thereof in the Fourier-transformed spectrograms in the frequency range of 1.5-3.5 kHz with frequency drifts on the order of 1 kHz/s.

- Secondary triggered emissions are sometimes observed to be triggered by the primary triggered emissions.

- Occasionally the principal triggered emissions are observed less than 1 s later at greatly reduced amplitudes.

- The triggered emissions are observed within about 20 degrees north and south of the magnetic equator at around 4-5 R_E, all magnetic local times, and L-shells of 4-6.

- Correlation distances are as great as about 800 km both along and cross B.

- The triggered emissions are seen propagating both toward and away from the magnetic equator at group velocities less than 1 x 10^8 m/s.

- The triggers appear to be hiss and narrowband, constant-frequency type emissions.

Cluster's orbit has proven to be very advantageous for obtaining observations of triggered emissions in the form of VLF risers, fallers and hooks since its perigee around 4 R_E is nearly at the magnetic equator and often cuts through at the plasmapause, or just inside or outside of it, at L-shells around 4-6. Thus, this orbit combined with the multi-spacecraft capability promises to provide even more discoveries and a greater understanding of these intense emissions and their connection to solar activity and changes in interplanetary magnetic fields.

Acknowledgments

This work was supported under NASA/Goddard Space Flight Center Grant No. NAG5-9974. We thank all of the many groups on the European side for their part in obtaining the WBD data (ESA, ESTEC, ESOC, JSOC, Sheffield University, and the Cluster Wave Experiment Consortium), as well as those on the U.S. side (JPL/DSN). We also thank ESA and NASA for valuable analysis support tools, namely, CSDSWeb, SSCWeb and CDAWeb). The authors also

wish to thank B.R Sandel and the IMAGE/EUV team at the University of Arizona for their assistance in the processing and analysis of EUV data.

References

André, M., Behlke, R., Wahlund, J.-E., Vaivads, A., Eriksson, A.-I., et al.: Multi-spacecraft observations of broadband waves near the lower hybrid frequency at the Earthward edge of the magnetopause, Ann. Geophys., 19, 1471-1481, 2001.

Balogh, A., Dunlop, M. W., Cowley, S. W. H., Southwood, D. J., Thomlinson, J. G., et al.: The Cluster Magnetic Field Investigation, Space Sci. Rev., 79, 65-92, 1997.

Bell, T. F.: High amplitude VLF transmitter signals and associated sidebands observed near the magnetic equatorial plane on the ISEE 1 satellite, J. Geophys. Re., 90, 2792-2795, 1985.

Bell, T. F., Inan, U. S., Helliwell, R. A., and Scudder, J. D.: Simultaneous triggered VLF emissions and energetic electron distributions observed on POLAR with PWI and HYDRA, Geophys. Res. Lett., 27(A2), 165-168, 2000.

Chappell, C.R., Harris, K. K. and Sharp, G. W.: The dayside of the plasmasphere, J. Geophys. Res., 76, 7632-7647, 1971.

Cornilleau-Wehrlin, N., Chauveau, P., Louis, S., Meyer, A., Nappa, J. M., et al.: The Cluster spatio-temporal analysis of field fluctuations (Staff) experiment, Space Sci. Rev., 79, 107-136, 1997.

Décréau, P. M. E., Fergeau, P., Krasnosels'kikh, V., Lévêque, M., Martin, Ph., et al.: WHISPER, a resonance sounder and wave analyser: performances and perspectives for the Cluster mission, Space. Sci. Rev., 79, 157-193, 1997.

Gurnett, D. A., Huff, R. L., and Kirchner, D. L.: The wide-band plasma wave investigation, Space Sci. Rev., 79, 195-208, 1997.

Gurnett, D. A., Huff, R. L., Picket, J. S., Person, A. M., Mutel, R. L., et al.: First results from the Cluster wideband plasma wave investigation, Ann. Geophys., 19, 1259-1272, 2001.

Gustafsson, G., Bostrom, R., Holback, B., Holmgren, G., Lundgren, A., et al.,: The electric field and wave experiment for the Cluster mission, Space Sci. Rev., 79, 137-156, 1997.

Helliwell, Robert A.: *Whistlers and related ionospheric phenomena*, Stanford University Press, Stanford, California, 1965.

Johnstone, A. D., Alsop, C., Burge, S., Carter, P. J., Coates, A. J., et al.: Peace: a plasma electron and current experiment, Space Sci. Rev., 79, 351-398, 1997.

Lauben, D. S., Inan, U. S., Bell, T. F., and Gurnett, D. A.: Source characteristics of ELF/VLF chorus, J. Geophys. Res., 107(A10), doi:10.1029/2000JA003019, 1429-1445, 2002.

LeDocq, M. J., Gurnett, D. A., and Hospodarsky, G. B.: Chorus source locations from VLF Poynting flux measurements with the Polar spacecraft, Geophys. Res. Lett., 25, 4063-4066, 1998.

Matsumoto, H.: Nonlinear whistler-mode interaction and triggered emissions in the magnetosphere: a review, in *Wave Instabilities in Space Plasmas*, Palmadesso, P. J. and Papadopoulos, K. (eds), D. Reidel, Dordrecht, 163-, 1979.

Meredith, N. P., Horne, R. B., and Anderson, R. R.: Substorm dependence of chorus amplitudes: implications for the acceleration of electrons to relativistic energies, J. Geophs. Res., 106, 13,165-13,178, 2001.

Moldwin, M.B., Thomsen, M. G., Bame, S. J., McComas, D. J., and Moore, K. R.: An examination of the structure and dynamics of the outer plasmasphere using multiple geosynchronous satellites, J. Geophys. Res., 99, 11,475-11,481, 1994.

Moldwin, M. B., Downward, L., Rassoul, K., Amin, R. and Anderson, R. R.: A new model of the location of the plasmapause: CRRES results, J. Geophys. Res., 107(A11), 1339, doi:10.1029/2001JA009211, 2002.

Nunn, D. and Smith, A. J.: Numerical simulation of whistler-triggered VLF emissions observed in Antarctica, J. Geophys. Res., 101(A3), 5261-5277, 1996.

Nunn, D., Omura, Y., Matsumoto, H., Nagano, I., and Yagitani, S., The numerical simulation of VLF chorus and discrete emissions observed on the Geotail satellite using a Vlasov code, J. Geophys. Res., 102(A12), 27,083-27,097, 1997.

Omura, Y., Nunn, D., Matsumoto, H. and Rycroft, M. J.: A review of observational, theoretical and numerical studies of VLF triggered emissions, J. Atmos. and Terres. Phys., 53(5), 351-368, 1991.

Parrot, M., Santolík, O., Cornilleau-Wehrlin, N., Maksimovic, M. and Harvey, C.: Magnetospherically reflected chorus waves revealed by ray tracking with CLUSTER data, Ann. Geophys., in press, 2003.

Pasmanik, D. L., Demekhov, A. G., Nunn, D., Trakhtengerts, V. Y., and Rycroft, M. J.: Cyclotron amplification of whistler-mode waves: A parametric study relevant to discrete VLF emissions in the Earth's magnetosphere, J. Geophys. Res., 107(A8), 10.1029/2001JA000256, 2002.

Pedersen, A., Decreau, P., Escoubet, C.-P., Gustafsson, G., Laakso, H., et al.: Four-point high time resolution information on electron densities by the electric field experiments (EFW) on Cluster, Ann. Geophys., 19, 1483-1489, 2001.

Sandel, B. R., Broadfoot, A. L., Curtis, C. C., King, R. A., Stone, T. C., et al.: The extreme ultraviolet imager investigation for the IMAGE mission, Space Sci. Rev., 91, 197-, 2000.

Sandel, B.R., King, R. A., Forrester, W. T., Gallagher, D. L., Broadfoot, A. L. and Curtis, C. C.: Initial results from the IMAGE extreme ultraviolet imager, Geophys. Res. Lett., 28, 1439, 2001.

Santolík, O and Gurnett, D. A.: Transverse dimensions of chorus in the source region, Geophys. Res. Lett., 30(2), 1031, doi:10.1029/2002GL016178, 2003.

Santolík, O., Lefeuvre, F., Parrot, M., and Rauch, J. L.: Complete wave-vector directions of electromagnetic emissions: Application to INTERBALL-2 measurements in the nightside auroral zone, J. Geophys. Res., 106, 13,191-13,201, 2001.

Santolík, O, Parrot, M., and Lefeuvre, F.: Singular value decomposition methods for wave propagation analysis, Radio Sci., 38(1), 1010, doi:10.1029/2000RS002523, 2003.

Sazhin, S. S. and Hayakawa, M.: Magnetospheric chorus emissions: A review, Planet. Space Sci., 40(5), 681-697, 1992.

Smith, A. J. and Nunn, D.: Numerical simulation of VLF risers, fallers, and hooks observed in Antarctica, J. Geophys. Res., 203(A4), 6771-6784, 1998.

Stix, T. H.: *Waves in Plasmas*, Am. Inst. of Phys., New York, 1992.

Trakhtengerts, V. Y.: A generation mechanism for chorus emission, Ann. Geophys., 17, 95-100, 1999.

Trakhtengerts, V. Y. and Rycroft, M.J.: Whistler-electron interactions in the magnetosphere: new results and novel approaches, J. Atmos. and Terres. Phys., 62, 1719-1733, 2000.

Figure Captions

Figure 1: Cluster WBD spectrogram of linked risers and fallers (or upward and downward hooks) observed on all four Cluster spacecraft on March 11, 2002. The hooks appear to be triggered out of a constant frequency wave of frequency about 2.8 kHz.

Figure 2: Electron density profile constructed using Cluster Whisper Sounder and EFW spacecraft potential measurements on March 11, 2002. The arrow indicates the time of the WBD measurements of triggered emissions, this being in the plateau or cavity region just after the first sharp density drop coming out of the plasmasphere.

Figure 3: Data from the IMAGE EUV instrument. a) The left-hand panel displays the image data taken soon after the time of the Cluster WBD measurements on March 11, 2002. The right-hand panel identifies the pertinent boundaries associated with the plasmasphere. b) The left-hand panel shows the location of Cluster with respect to those boundaries at the time of the IMAGE measurements. The right-hand panel shows the location of Cluster with respect to those boundaries with the IMAGE data co-rotated back to the time of the Cluster measurements.

Figure 4: Cluster WBD spectrogram of riser/hook combinations observed on June 23, 2003 on two Cluster spacecraft. The riser/hook combinations appear to be triggered out of the hiss that cuts off around 2 kHz.

Figure 5: FIR-filtered waveform in the frequency band of 2-3 kHz of the riser/hook combination observed around 03:45:13 on June 23, 2003. Note the good correlations of the waveforms across the two spacecraft, which are used to obtain a time delay. In this case the riser/hook combination is seen first on SC2.

Figure 6: Electron density profile constructed using Whisper Sounder and EFW spacecraft potential measurements on June 23, 2003. The arrow indicates the time of the WBD measurements of triggered emissions, this being inside a broader localized density cavity in or near the plasmapause.

Figure 7: Time-frequency spectrograms measured by the STAFF-SA instrument onboard SC2 on June 23, 2003. (a) Sum of the power spectral densities of the two orthogonal electric components in the spin plane of the spacecraft. (b) Sum of the power spectral densities of the three orthogonal magnetic components. (c) Angle between the wave vector and the stationary magnetic field obtained from the cross-spectral analysis of the magnetic components using the SVD method. (d) Estimate of the electromagnetic planarity of wave fluctuations obtained using the SVD analysis. (e) Parallel component of the Poynting flux normalized by its standard deviation. Position of the spacecraft is given on the bottom, MLat being

the magnetic dipole latitude in degrees, MLT being the magnetic local time in hours, and R being the radial distance in Earth radii.

Figure 8: Cluster WBD spectrogram of risers observed on August 31, 2003 on all four Cluster spacecraft. The risers appear to be triggered out of the hiss.

Figure 9: Electron density profile constructed using Cluster Whisper Sounder and EFW spacecraft potential measurements on August 31, 2003. The arrow indicates the time of the WBD measurements of the risers, this occurring on the steep density gradient on plasmasphere entry.

Event Number	Correlation Event Time		Delay Time (s)
	SC2 (UT)	SC4 (UT)	
1	03:45:13.10839	03:45:13.11284	0.00445
2	03:45:13.21639	03:45:13.21990	0.00351
3	03:45:13.36511	03:45:13.36839	0.00328
4	03:45:13.40467	03:45:13.40767	0.00300

Table 1: Delay times associated with event times shown in Figure 5.

	SC1-SC2 (km)	SC1-SC3 (km)	SC1-SC4 (km)	SC2-SC3 (km)	SC2-SC4 (km)	SC3-SC4 (km)
Mar. 11, 2002						
// to B	105	162	216	57	111	54
$\perp$ to B	151	195	306	71	166	111
Jun. 23, 2003						
// to B					266	
$\perp$ to B					239	
Aug. 31, 2003						
// to B	464	560	825	96	361	265
$\perp$ to B	518	421	747	98	243	333

Table 2: Spacecraft separations along and across B for time periods shown in Figures 1, 4 and 8.

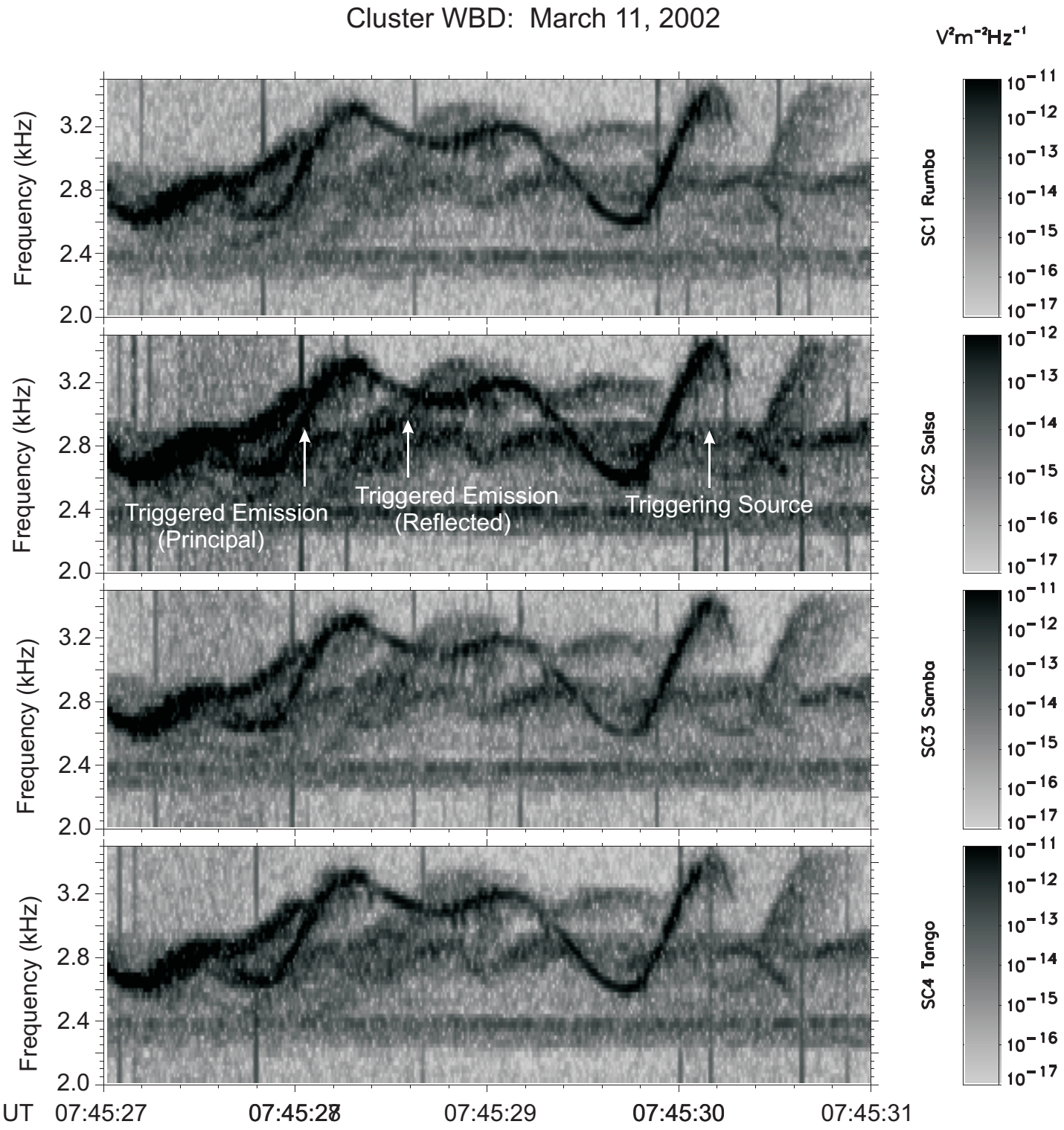
Cluster WBD: March 11, 2002
V²m⁻²Hz⁻¹
Frequency (kHz)
3.2
2.8
2.4
2.0
SC1 Rumba
SC2 Salsa
SC3 Samba
SC4 Tango
10⁻¹¹
10⁻¹²
10⁻¹³
10⁻¹⁴
10⁻¹⁵
10⁻¹⁶
10⁻¹⁷
Triggered Emission (Principal)
Triggered Emission (Reflected)
Triggering Source
UT
07:45:27
07:45:28
07:45:29
07:45:30
07:45:31

Figure 1

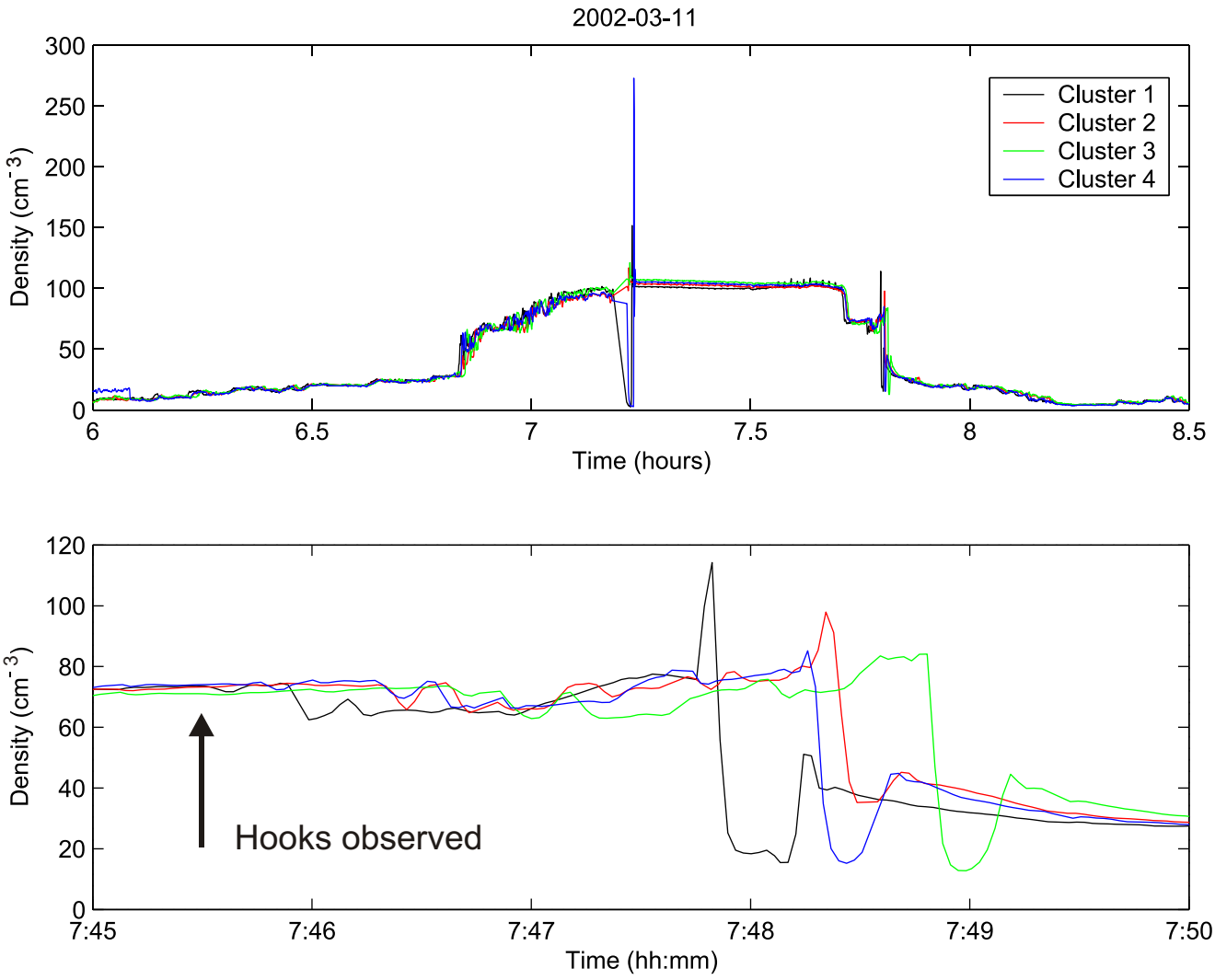
2002-03-11
Density (cm-3)
Time (hours)
Cluster 1
Cluster 2
Cluster 3
Cluster 4
Hooks observed
Time (hh:mm)

Figure 2

(a)

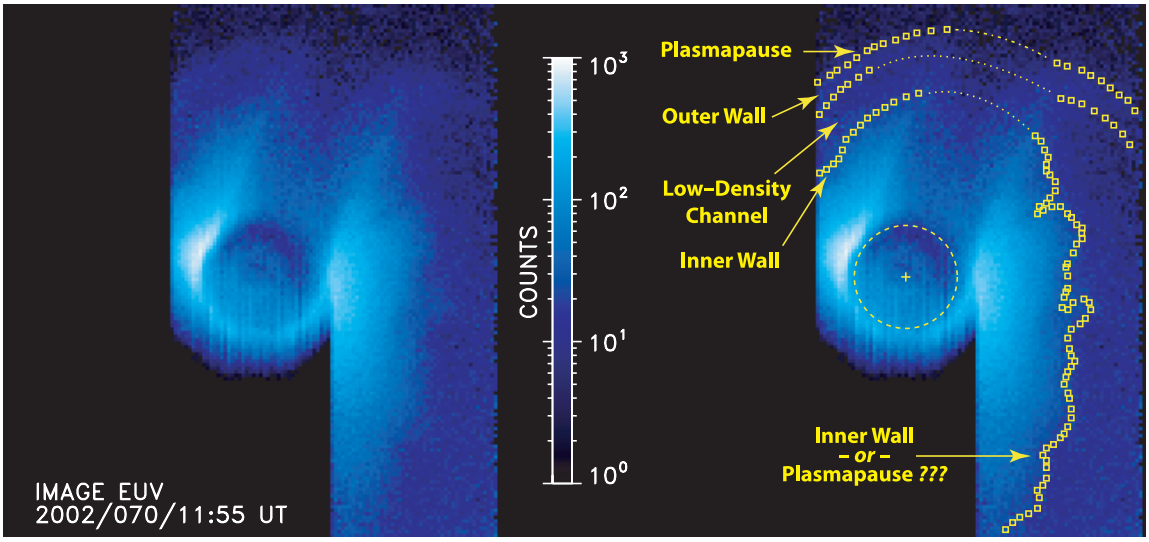
IMAGE EUV
2002/070/11:55 UT
COUNTS
10^3
10^2
10^1
10^0
Plasmapause
Outer Wall
Low-Density Channel
Inner Wall
Inner Wall
– or –
Plasmapause ???

(b)

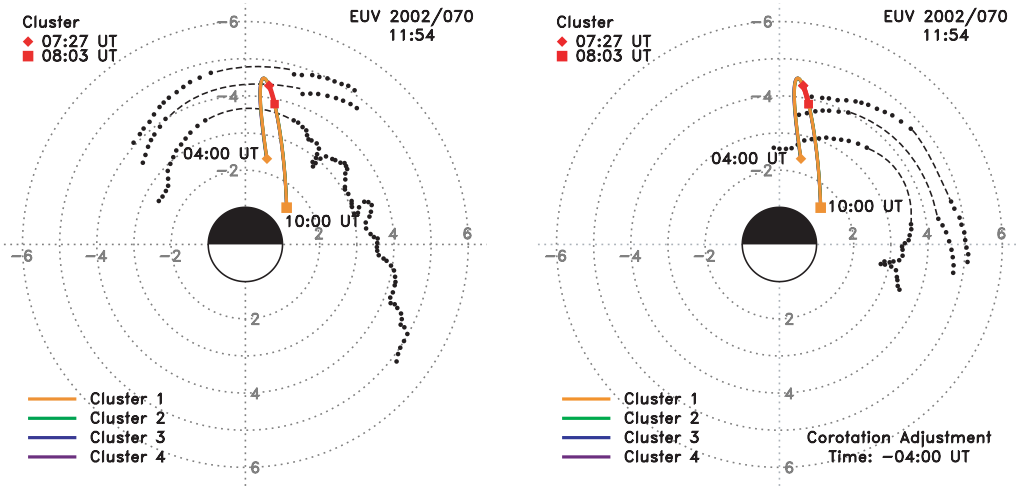
Cluster
07:27 UT
08:03 UT
EUV 2002/070
11:54
04:00 UT
10:00 UT
Cluster 1
Cluster 2
Cluster 3
Cluster 4
Cluster
07:27 UT
08:03 UT
EUV 2002/070
11:54
04:00 UT
10:00 UT
Cluster 1
Cluster 2
Cluster 3
Cluster 4
Corotation Adjustment
Time: −04:00 UT

Figure 3

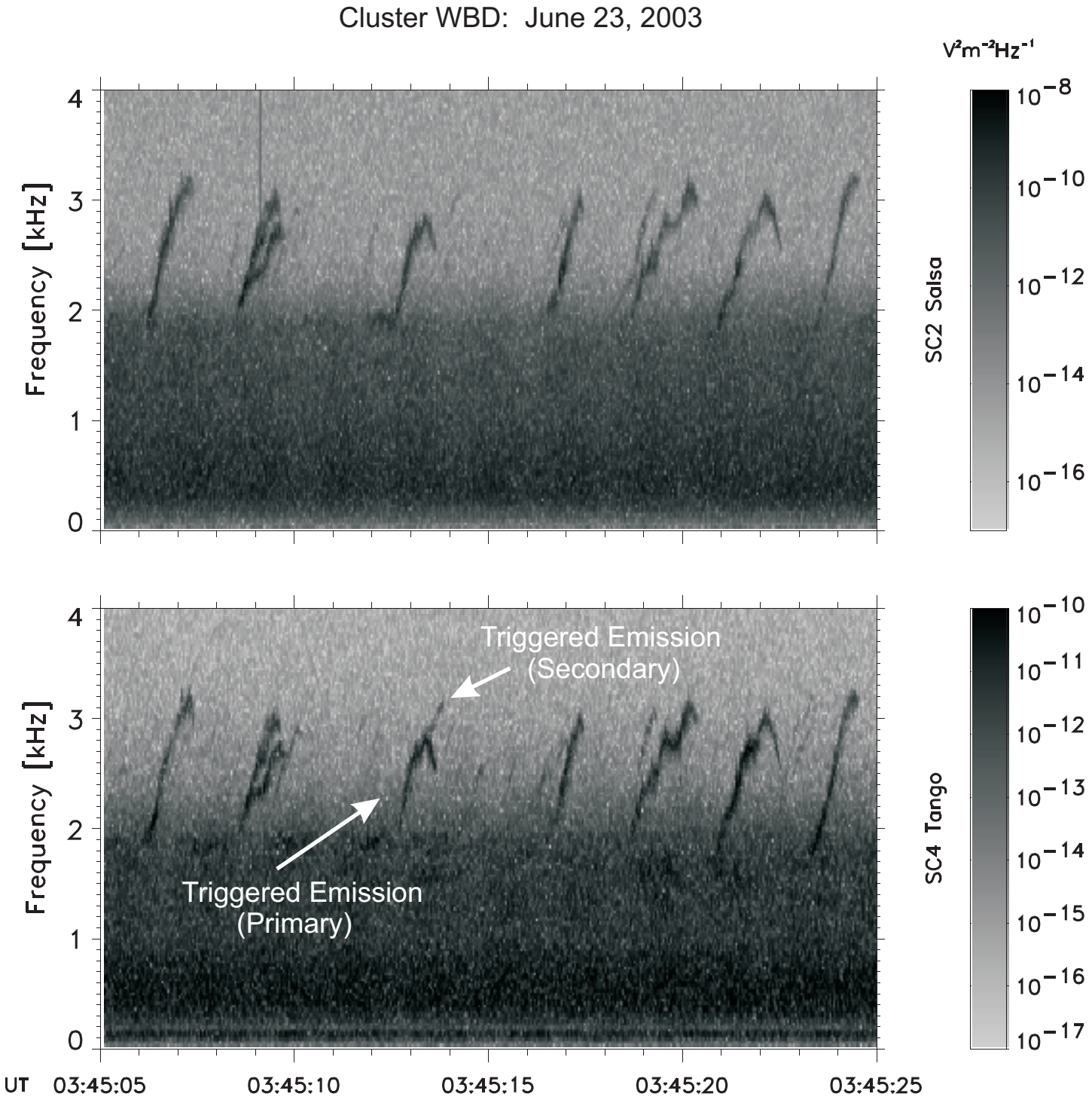
Cluster WBD: June 23, 2003
V²m⁻²Hz⁻¹
Frequency [kHz]
4
3
2
1
0
SC2 Salsa
10⁻⁸
10⁻¹⁰
10⁻¹²
10⁻¹⁴
10⁻¹⁶
Triggered Emission
(Secondary)
Triggered Emission
(Primary)
SC4 Tango
10⁻¹⁰
10⁻¹¹
10⁻¹²
10⁻¹³
10⁻¹⁴
10⁻¹⁵
10⁻¹⁶
10⁻¹⁷
UT
03:45:05
03:45:10
03:45:15
03:45:20
03:45:25

Figure 4

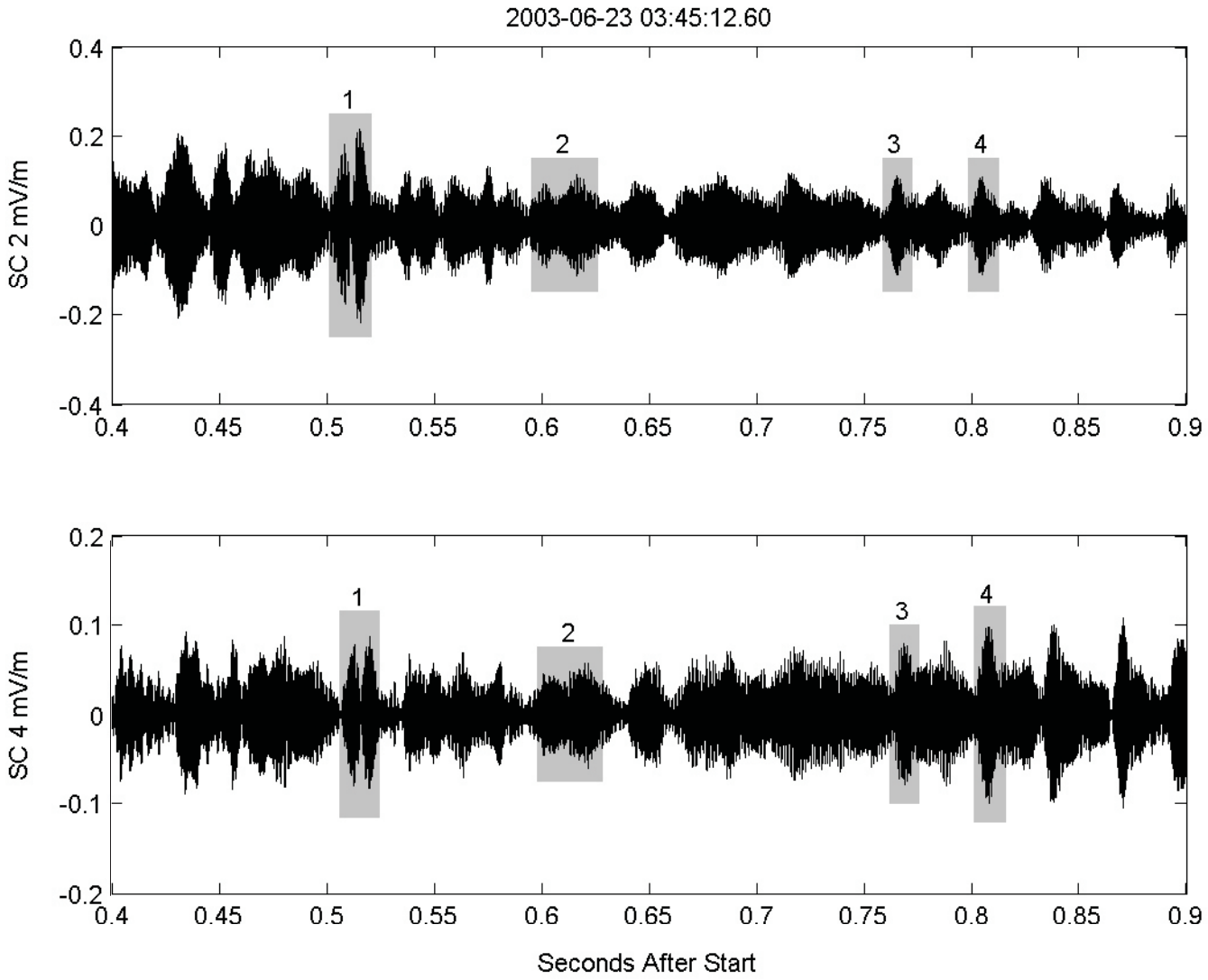

Figure 5

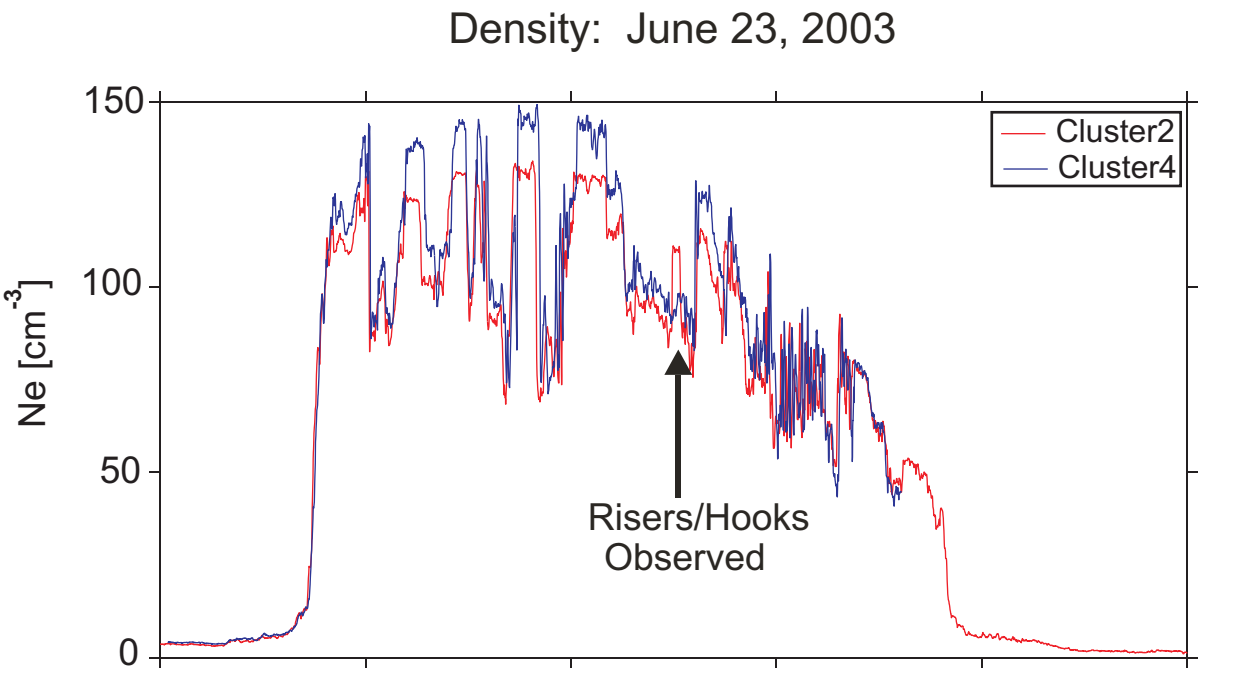

UT	02:30	03:00	03:30	04:00	04:30	05:00
R(R_E)	4.97	4.66	4.47	4.43	4.55	4.80
MLAT(°)	-23.58	-10.21	4.78	20.62	36.15	50.35
MLT	17:15	17:04	16:53	16:40	16:26	16:09
L	5.92	4.81	4.50	5.06	6.97	11.79

Figure 6

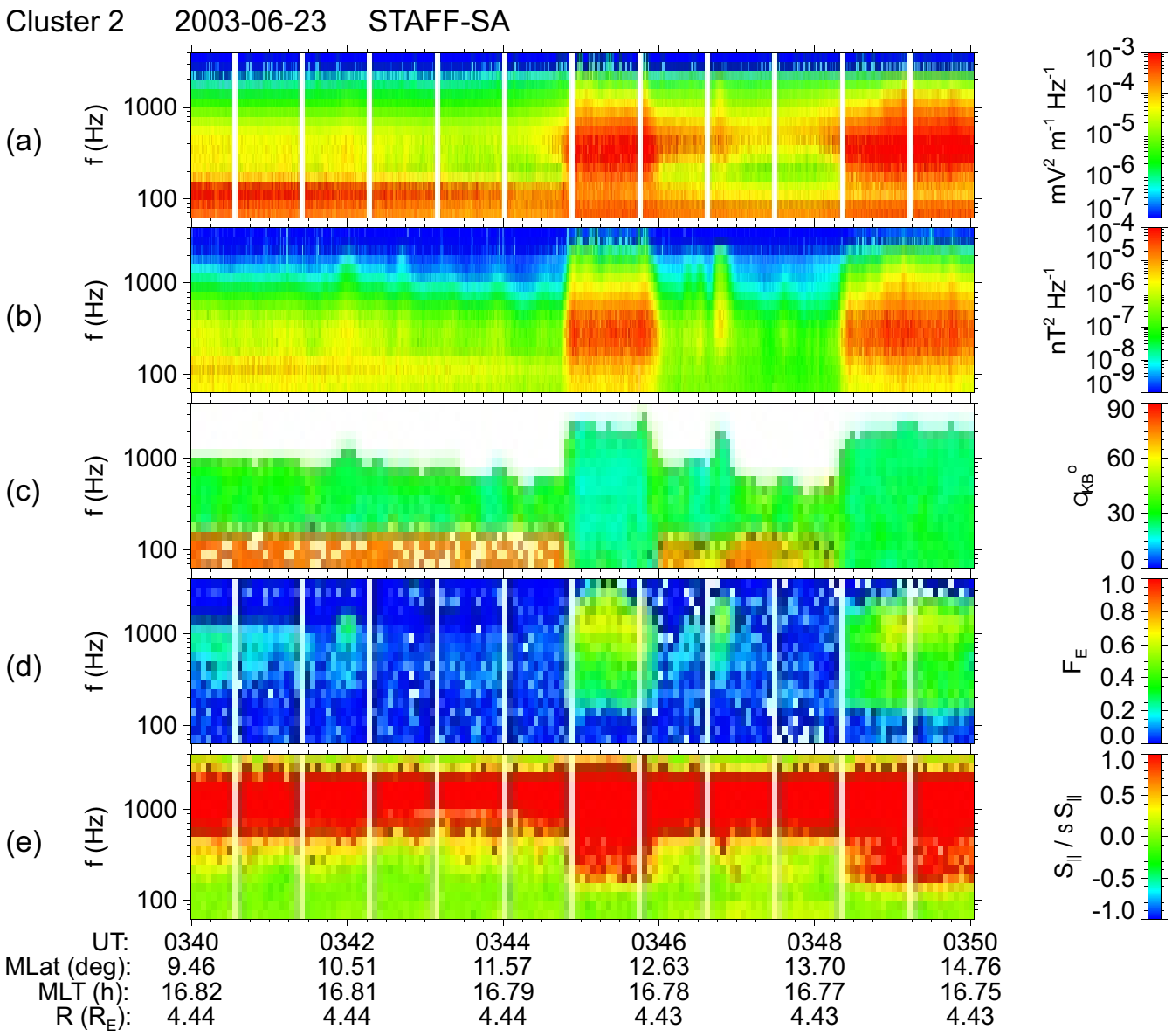
Cluster 2 2003-06-23 STAFF-SA
(a)
(b)
(c)
(d)
(e)
f (Hz)
1000
100
mV² m⁻¹ Hz⁻¹
nT² Hz⁻¹
θkB °
FE
S|| / s S||
UT: 0340 0342 0344 0346 0348 0350
MLat (deg): 9.46 10.51 11.57 12.63 13.70 14.76
MLT (h): 16.82 16.81 16.79 16.78 16.77 16.75
R (RE): 4.44 4.44 4.44 4.43 4.43 4.43

Figure 7

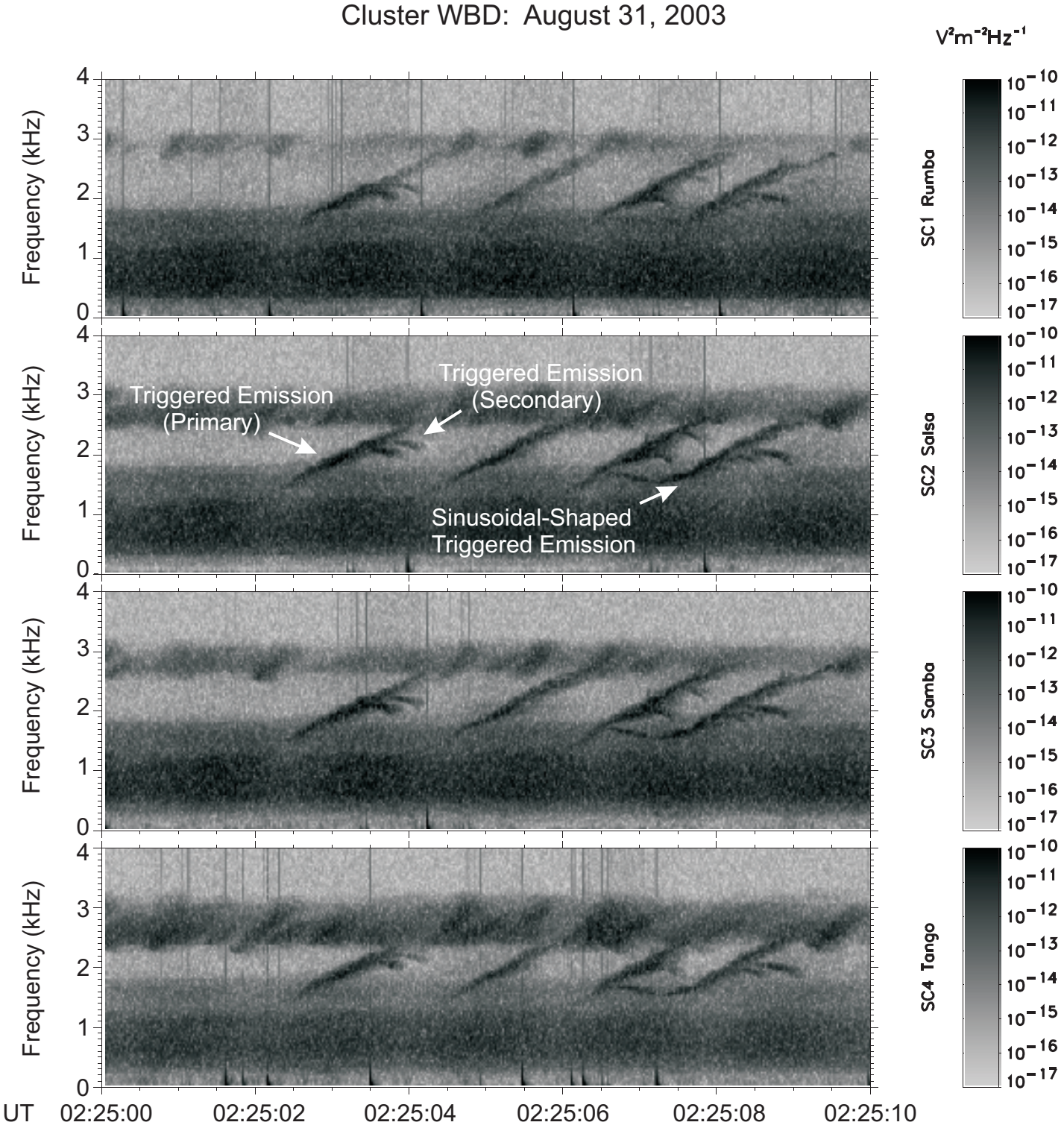
Cluster WBD: August 31, 2003
V²m⁻²Hz⁻¹
Frequency (kHz)
Triggered Emission (Primary)
Triggered Emission (Secondary)
Sinusoidal-Shaped Triggered Emission
SC1 Rumba
SC2 Salsa
SC3 Samba
SC4 Tango
UT
02:25:00
02:25:02
02:25:04
02:25:06
02:25:08
02:25:10

Figure 8

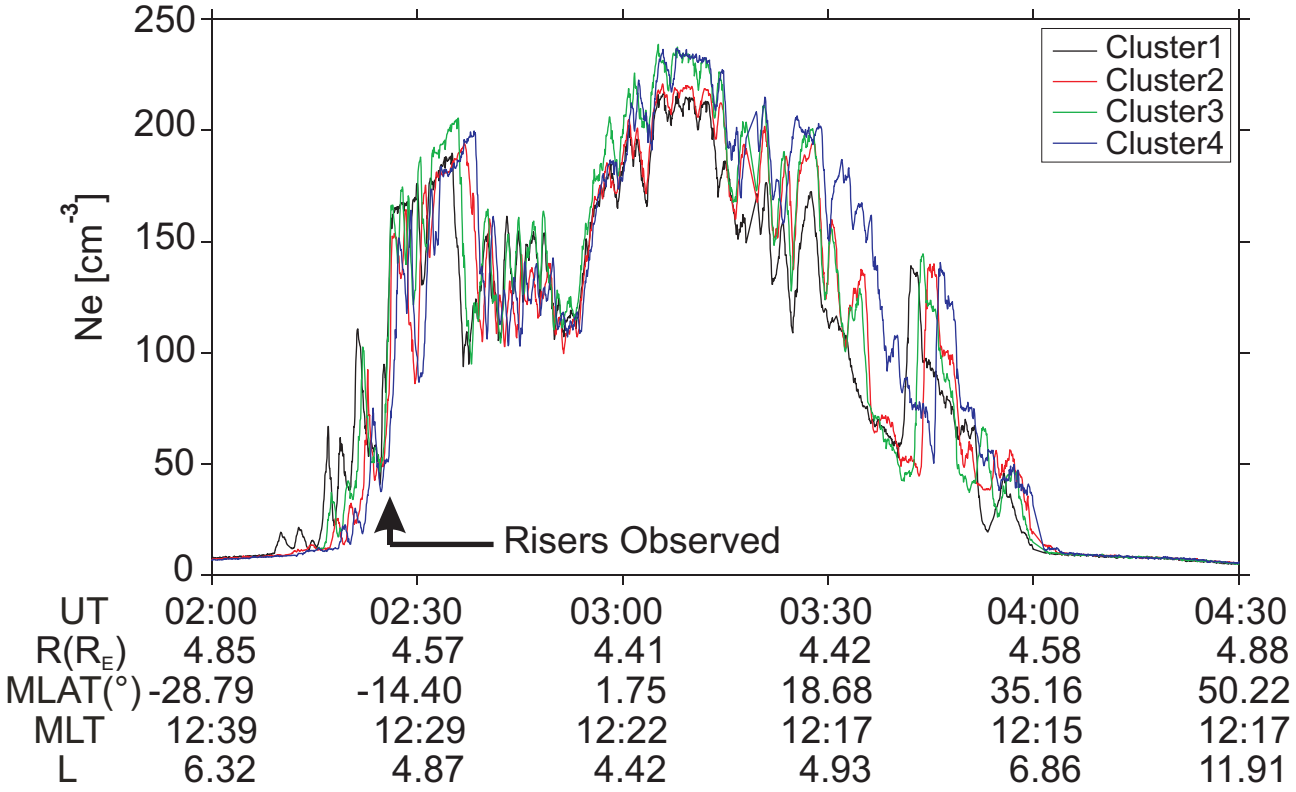
Density: August 31, 2003
250
200
150
100
50
0
Ne [cm-3]
Cluster1
Cluster2
Cluster3
Cluster4
Risers Observed
UT 02:00 02:30 03:00 03:30 04:00 04:30
R(RE) 4.85 4.57 4.41 4.42 4.58 4.88
MLAT(°) -28.79 -14.40 1.75 18.68 35.16 50.22
MLT 12:39 12:29 12:22 12:17 12:15 12:17
L 6.32 4.87 4.42 4.93 6.86 11.91

Figure 9